PHYSICAL REVIEW D **90,** 126011 (2014)

Glueball instability and thermalization driven by dark radiation

Kazuo Ghoroku,[1,*] Masafumi Ishihara,[2,†] Akihiro Nakamura,[3,‡] and Fumihiko Toyoda[4,§]

[1]*Fukuoka Institute of Technology, Wajiro, Higashi-ku, Fukuoka 811-0295, Japan*
[2]*WPI-Advanced Institute for Materials Research (WPI-AIMR), Tohoku University, Sendai 980-8577, Japan*
[3]*Department of Physics, Kagoshima University, Korimoto1-21-35, Kagoshima 890-0065, Japan*
[4]*Faculty of Humanity-Oriented Science and Engineering, Kinki University, Iizuka 820-8555, Japan*

(Received 12 July 2014; published 24 December 2014)

We study glueballs in the holographic gauge theories living in a curved space-time. The dual bulk is obtained as a solution of the type IIB superstring theory with two parameters, which correspond to the four-dimensional cosmological constant λ and the dark radiation C, respectively. The theory is in the confining phase for $\lambda < 0$ and small C, then we observe stable glueball states in this theory. However, the stability of the glueball states is lost when the density of the dark radiation (C) increases and exceeds a critical point. Above this point, the dark radiation works as the heat bath of the Yang-Mills theory since the event horizon appears. Thus the system is thermalized, and the theory is in a finite temperature deconfinement phase, namely in the QGP phase. We observe this transition process through the glueball spectra which varies dramatically with C. We also examined the entanglement entropy of the system to find a clue of this phase transition and the role of the dark radiation C in the entanglement entropy.

DOI: 10.1103/PhysRevD.90.126011 PACS numbers: 11.25.Tq, 11.10.Wx, 11.15.-q, 12.38.Aw

I. INTRODUCTION

The holographic approach is a powerful method to study the nonperturbative properties of the strong coupling gauge theories [1–3]. In this context, various attempts have been performed to study the properties of the supersymmetric Yang Mills (SYM) theory. While most of these approaches have been performed for the four-dimensional theory living in the Minkowski space-time, the analysis has been extended to the theory living in the Friedmann-Robertson-Walker (FRW) type space-time [4–10]. In this case, two free parameters, the four-dimensional cosmological constant (λ) and the dark radiation (C), have been introduced in the asymptotic AdS_5 solution.

Due to the parameter λ, the boundary geometry is changed from the Minkowski to $dS_4(AdS_4)$ space-time for $\lambda > 0(\lambda < 0)$. Then this solution opens the way to the holographic approach to the SYM theory in the curved space-time. In the present case, it has been cleared that the dynamical properties of the SYM theory is largely influenced by the geometry of the boundary as shown in [4,5] and [6] for dS_4 and AdS_4, respectively. Especially, in the case of $\lambda < 0$ or AdS_4 boundary, it has been found that the theory is in the confining phase [6].

As for the dark radiation, on the other hand, it has been introduced in the context of the Randall-Sundrum brane-world cosmology [11,12]. In the context of the brane world model, this term has been regarded as the projection of the five-dimensional Weyl term on the four-dimensional brane [13,14]. From the holographic viewpoint, however, this term should be identified with the thermal excitation of SYM fields as observed in the limit of $\lambda = 0$ [7–10]. For $\lambda = 0$, the bulk configuration with C is expressed by the Schwaltzschild-AdS_5 by a redefinition of the radial coordinate, and then we find the Hawking temperature which is proportional to C [7]. It is well known that this configuration is dual to the finite temperature SYM theory in deconfinement phase.

The dark radiation C therefore competes with the negative λ in the dynamics of the SYM theory. Namely, C prevents the realization of the confinement phase which is supported by the negative λ. In this paper, the competition of these parameters is examined by using r_0 and b_0, which are defined by (2.8) and (2.7) in the next section, instead of λ and C, respectively. So the point mentioned above could be expressed by a critical line in the parameter plane of $b_0 - r_0$ (see the next section) of the quark confinement-deconfinement phase transition as has been discussed in [7,9,10]. As shown in [7], we should notice that b_0 varies with time through the scale factor $a_0(t)$ of the FRW metric even if C is fixed at some finite value. In the case of negative λ, we have a solution of $a_0(t)$ which oscillates between -1 and $+1$. Then the phase transition of confinement-deconfinement is observed during the time-interval of this oscillation. We however investigate here the transition within a small time-interval under the assumption $\dot{a}_0(t)/a_0(t) \ll 1$. In this case, the transition is caused by the change of C.

In the deconfinement phase, for large b_0, the dark radiation would be identified with the thermal YM fields

*gouroku@dontaku.fit.ac.jp
†masafumi@wpi-aimr.tohoku.ac.jp
‡k3880508@kadai.jp
§ftoyoda@fuk.kindai.ac.jp

or the exited gluons as mentioned above. On the other hand, one may wonder what kind of object is identified with this dark radiation in the confinement phase for small b_0. In order to resolve this point, we here study more about this phase transition through the glueball spectra since it may be related to the dark radiation in the confinement phase with finite b_0.

Here we should point out another characteristic point observed for negative λ case. It is the second boundary in the infrared side of the bulk as discussed in [10]. In the case of zero and small b_0, in the confinement phase, there is no special point like horizon in the bulk between the two boundaries, which are both described by AdS_4. It would be related to the fact that the two AdS_4 are connected for $C = 0$ at their three-dimensional boundary, which are described by three-dimensional hyperbolic space H^3, [15,16]. Then the field operators living on each AdS_4 space-time would extend to the other AdS_4. This behavior of the field operators would be observed in the bulk in some way, then we expect to be able to see it through the holographic analysis.

For the case of $C = 0$, we actually find that the metric of the bulk is symmetric under an inversion transformation ($z = r_0^2/r$) of the fifth coordinate (r) at a point $r = r_0$. We call the four-dimensional slice at this point the "domain wall" since the existing region of the strings and the branes introduced as probes to investigate the dynamics of the dual theory is restricted to the range $r_0 < r < \infty$ or $0 < r < r_0$.[1] This point has been discussed in [10]. Then the bulk is separated to two regions by this domain wall. Then we expect to find the equivalence of the theory on the boundary $r = \infty$ and the one at $r = 0$ for $C = 0$.

For $C \neq 0$, the position of the domain walls is changed depending on the quantities to be studied. The wall for the static string, which is used to see the string tension responsible to the quark confinement, and for the entanglement entropy are shown as such examples. They are at the same point for $C = 0$, then we can see how they vary with increasing b_0. After the transition to the deconfinement phase at large b_0, a horizon appears and the second boundary is hidden behind the horizon.

On the other hand, the dual of the glueballs are examined through the fluctuation of the bulk fields or as rotating closed string configurations. When we observe the fluctuation of the fields, the domain wall seems to be disappearing since the wave function of the fluctuation spreads out all over the bulk. However, we could see that the center of the wave function of the glueball state and the classical configuration of rotating closed string are just on the domain wall. In this sense, the role of the domain wall is altered in the glueball case. The glueballs are attracted at the domain wall and they could spread as the quantum fluctuations as shown below. The situation depends on the dark radiation C. The glueballs can be observed in both theories on the opposite side boundaries.

The outline of this paper is as follows. In the next section, the bulk solutions for our holographic model are given, then some important points are briefly reviewed. In Sec. III, the spectra of glueballs in the case of $C = 0$ are shown as an exact form of analytical solution. Also, the spectrum for $C \neq 0$ is estimated by WKB approximation for the lowest mass of the glueball to see its behavior near the transition point to the deconfinement phase. In Sec. IV, the glueballs with higher mass state are examined by solving the equation of motion for the rotating closed string with folding form. We could show that the properties of the solutions for $C \neq 0$ are consistent with the one given in the previous section. In Sec. V, the entanglement entropy has been examined and we could find the thermal limit of the dark radiation part in the deconfinement phase for large volume limit of the considering minimal surface. Other interesting properties are also given and discussed. The summary and discussions are given in the final section.

II. GRAVITY DUAL OF DARK ENERGY AND DARK RADIATION

The holographic dual to the large N gauge theory embedded in a space-time with dark energy and dark radiation is solved by the gravity on the following form of the metric

$$ds_{10}^2 = \frac{r^2}{R^2}(-\bar{n}^2 dt^2 + \bar{A}^2 a_0^2(t)\gamma_{ij}(x)dx^i dx^j) + \frac{R^2}{r^2}dr^2 + R^2 d\Omega_5^2, \tag{2.1}$$

where

$$\gamma_{ij}(x) = \delta_{ij}\left(1 + k\frac{\bar{r}^2}{4\bar{r_0}^2}\right)^{-2}, \qquad \bar{r}^2 = \sum_{i=1}^{3}(x^i)^2, \tag{2.2}$$

and $k = \pm 1$, or 0. The arbitrary scale parameter $\bar{r_0}$ of three spae is set hereafter as $\bar{r_0} = 1$. The solution is obtained from ten-dimensional supergravity of type IIB theory [7–10]. A brief review is given in Appendix A.

The resulting solution is obtained as

$$\bar{A} = \left(\left(1 - \frac{\lambda R^2}{4}\left(\frac{R}{r}\right)^2\right)^2 + \tilde{c}_0\left(\frac{R}{r}\right)^4\right)^{1/2}, \tag{2.3}$$

$$\bar{n} = \frac{(1 - \frac{\lambda R^2}{4}(\frac{R}{r})^2)^2 - \tilde{c}_0(\frac{R}{r})^4}{\sqrt{(1 - \frac{\lambda R^2}{4}(\frac{R}{r})^2)^2 + \tilde{c}_0(\frac{R}{r})^4}}, \tag{2.4}$$

$$\tilde{c}_0 = CR^2/(4a_0^4), \tag{2.5}$$

[1] This position of the coordinate has been also noticed as a node of the wormhole in a slightly different context of holography for two boundary theories [16].

where the dark radiation C is introduced as an integral constant in solving the equation of motion (A6). On the other hand, the "dark energy" (or cosmological term) $\lambda(t)$ is introduced as follows:

$$\left(\frac{\dot{a}_0}{a_0}\right)^2 + \frac{k}{a_0^2} = \lambda. \tag{2.6}$$

While it is possible to extend λ to the time dependent form $\lambda(t)$ as in [7], we consider here the case of constant λ for simplicity. In the following, our discussion would be restricted to the case of negative constant λ and we assume very small time derivative of $a_0(t)$. For the sake of the justification of our assumption for $a_0(t)$, we should say that the solution $a_0 =$ constant is allowed for negative constant λ when we take $k = -1$.

The physical meaning of λ is clear, however the dark radiation C is not familiar. So we explain it here. For $\lambda = 0$, the meaning of C is clearly understood. In this case, the above five-dimensional metric is rewritten into the AdS-Schwartzschild form, then we find the Hawking temperature T_H as follows [7]:

$$T_H = \frac{\sqrt{2}b_0}{\pi R^2}, \qquad b_0 = \tilde{c}_0^{1/4} R. \tag{2.7}$$

This implies that the dark radiation C corresponds to the thermal radiation of SYM fields in the Minkowski space-time since $\lambda = 0$. It is also assured from the VEV of energy momentum tensor that the dark radiation corresponds to a perfect fluid of gluons (or radiation) with the temperature T_H [7].

A. Confinement-deconfinement phase transition

Therefore, when the dark radiation C is added in some way to the YM theory in the confinement phase, the confinement force is screened and the phase of the theory is changed to the deconfinement above a critical value of C. This phenomenon has been observed in the AdS_4 space-time by examining the Wilson loop [7]. It has been observed that the SYM system in the AdS_4 is in the confinement phase [5]. However, as mentioned above, the phase of the theory is changed to the deconfinement one with finite temperature by adding C, which satisfies the condition $b_0 > r_0$, where

$$r_0 = \frac{R^2}{2}\sqrt{|\lambda|}. \tag{2.8}$$

In this region, a horizon appears at $r = r_H$ which is given as

$$r_H = \sqrt{b_0^2 - r_0^2}. \tag{2.9}$$

Then in the AdS_4 space-time or for $\lambda < 0$ the phase transition occurs at $b_0 = r_0$, where the temperature is zero, namely $T_c = 0$. We notice that the temperature is zero in the range of confinement, $0 \le b_0 \le r_0$, and the temperature appears for $r_0 < b_0$, in the deconfinement region. The critical point $T_c = 0$ is represented therefore by the line $b_0 = r_0$ in the plane of $\lambda - b_0$ as shown in the Fig. 1.

Usually, this kind of transition is studied through the Hawking-Page transition by using two independent solutions, confinement solution and the one of the deconfinement. Then the Hawking-Page transition has been studied by comparing the free energy of the theories at a finite temperature for those two bulk solutions [17–20]. Then we find a critical temperature as a finite value.

In the present case, the phase transition is examined in terms of the same solution by varying b_0 instead of the temperature. In this sense, the present model is a new type

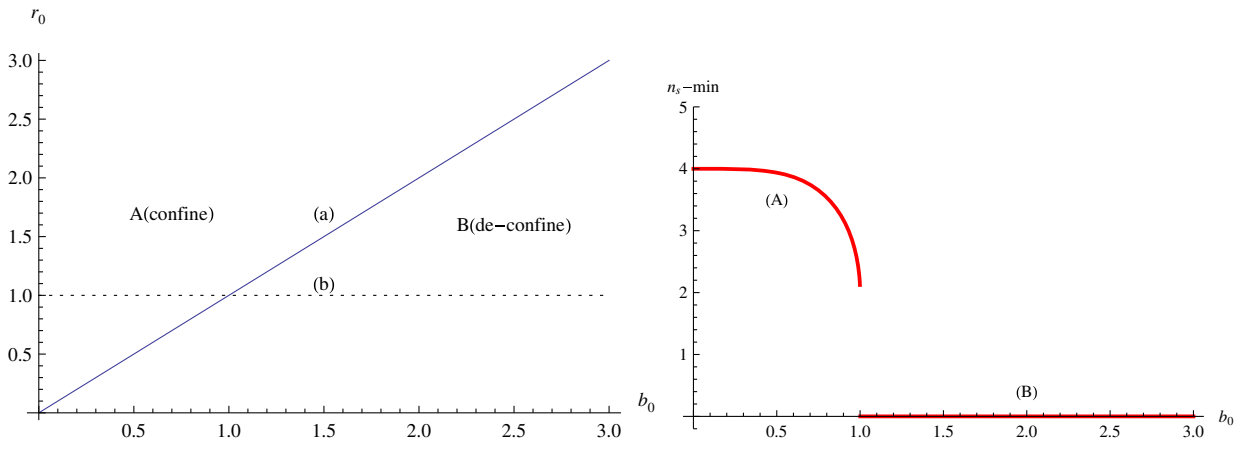

FIG. 1 (color online). Left: Phases for (A) quark confinement and (B) deconfinement are shown in $r_0 - b_0$ plane. The critical line $r_0 = b_0$ is shown by (a). Right: Minimum value of n_s is denoted by $n_{s-\min}$ and shown as a function of b_0 for $R = r_0 = 1$ along the vertical line (b) in the left figure. At the critical point $b_0 = 1$, we find a gap between the values of $n_{s-\min}(b_0 \to 1_-) = 2$ in the region (A) and $n_{s-\min}(b_0 \to 1_+) = 0$ in the region (B).

of holographic model. Our purpose is to study through this model the phase transition phenomenon in more detail.

In this transition, we could consider the QCD string tension as the order parameter. This point is briefly shown below under an assumption that the time evolution of the universe is very slow, or equivalently for $\dot{a}(t)/a_0(t) \ll 1$.

Here we should comment on the time dependence of b_0 in the above discussion. While we used b_0 given by (2.7) instead of the parameter C, b_0 includes the time-dependent scale factor $a_0(t)$. So it is possible to see the phase transition at a fixed C when the enough time interval is taken [7]. We, however, consider here the transition in a rather small time interval under the above assumption $\dot{a}(t)/a_0(t) \ll 1$. So the value of C should be changed largely corresponding to the change of b_0 near the transition point.

1. QCD string tension as an order parameter

The potential between quark and antiquark is studied by the Wilson-Loop for the present case [7]. It is obtained holographically from the U-shaped (in $r-x$ plane) string which is embedded in the bulk and its two end points are on the boundary. Supposing a string whose world volume is set in (t, x) plane,[2] the energy E of this state is obtained as a function of the distance (L) between the quark and antiquark according to [5].

Taking the gauge as $X^0 = t = \tau$ and $X^1 = x^1 = \sigma$ for the coordinates (τ, σ) of string world volume, the Nambu-Goto action in the present background (A4) becomes

$$S_{\rm NG} = -\frac{1}{2\pi\alpha'}\int dtd\sigma\bar{n}(r)\sqrt{r'^2 + \left(\frac{r}{R}\right)^4(\bar{A}(r)a_0(t)\gamma(x))^2}, \tag{2.10}$$

where

$$\gamma(x) = \frac{1}{1-x^2/4}, \tag{2.11}$$

and we notice $r' = \partial r/\partial x = \partial r/\partial\sigma$. Here we notice the metric $\bar{n}$ and $\bar{A}$ have time dependence through $\tilde{c}_0$ as given above. As mentioned above, we must remember our assumption that the time derivative of $a_0(t)$ is very small compared to the time scale of the fields we are considering in the theory. So we could neglect this time dependence hereafter.

From the above action, $S_{\rm NG}$, the string configuration for large x is obtained by solving the equation of motion. Using this solution, we can estimate $S_{\rm NG}$. Then the linear potential is obtained when the factor n_s, which is given as

$$n_s = \left(\frac{r}{R}\right)^2\bar{A}\,\bar{n}, \tag{2.12}$$

has a minimum at some point of $r(=r_D>0)$. Further this minimum must be positive, $n(r_D) > 0$.

In the present case, such a point is found as

$$r_D = (r_0^4 - b_0^4)^{1/4}, \tag{2.13}$$

where $b_o = \tilde{c}_0^{1/4}R$ and

$$n_s(r_D) = 2\frac{r_0^2}{R^2}\left(1 + \frac{r_D^2}{r_0^2}\right). \tag{2.14}$$

Then, as shown in the Fig. 1, the positive minimum exists in the region,

$$r_0 \geq b_0 \geq 0. \tag{2.15}$$

We notice that there is a gap for the minimum of n_s at the transition point, $r_D = 0$. From (2.14), it is given as

$$n_s(0) = 2r_0^2/R^2, \tag{2.16}$$

which is finite. On the other hand, for $b_0 > r_0$, the horizon appears at $r = r_H$, which is given as

$$r_H = \sqrt{b_0^2 - r_0^2}. \tag{2.17}$$

Then, as shown in the Fig. 2, the minimum of $n_s(\geq 0)$ is given at this point as

$$n_s(r_H) = 0, \tag{2.18}$$

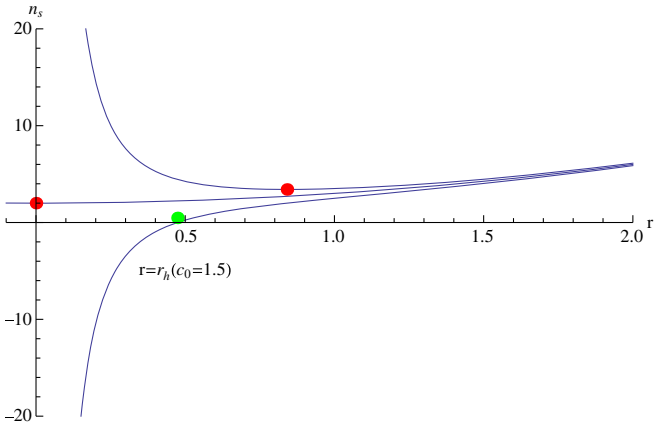

FIG. 2 (color online). The n_s is plotted as functions of r. The value of $\tilde{c}_0$ is 0.5, 1, 1.5 from the above. There $r_0 = 1, R = 1$ and $\lambda = -4r_0^2/R^4 = -4$. The red points are minimum points of n_s for $\tilde{c}_0 = 0.5$ and 1.0. The green point is the horizon at $\tilde{c}_0 = 1.5$.

[2]Here x denotes one of the three coordinate x^i, and we take x^1 in the present case.

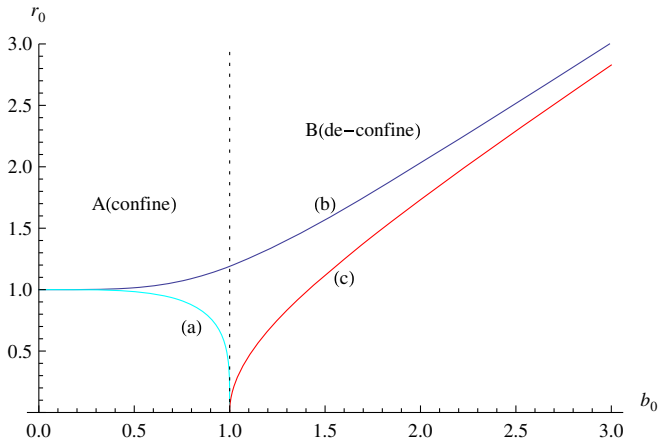

FIG. 3 (color online). Two dual bulks are shown in in $r - b_0$ plane. The domain wall is shown by the curve (a) $r_D = (r_0^4 - b_0^4)^{1/4}$ for $r_0 = 1$. The curve (c) denotes the horizon $r_H = \sqrt{-r_0^2 + b_0^2}$. The curve (b) $r_c = (r_0^4 + b_0^4)^{1/4}$ is explained in Sec. V. The vertical line shows the critical line for the confinement-deconfinement phase transition.

for $b_0 > 1$.[3] A typical case for $\tilde{c}_0 = 1.5$ is shown in the Fig. 2. For all range of $\tilde{c}_0$, the value of minimum of n_s is shown in the Fig. 1. This implies a gap for the string tension at the critical point. This fact implies the first order phase transition.

Domain wall.—We comment on the terminology "domain wall" related to the point r_D, where n_s takes its minimum. We call the four-dimensional slice, which is cut at $r = r_D$ in the bulk, a domain wall since the open string configuration introduced to calculate the string tension as above is prevented to penetrate this wall [10,21]. Then the bulk is separated by this wall to two regions in the case of $0 < b_0 < r_0$ as shown in Fig. 3. We could see that each region is dual to the four-dimensional field theory on each boundaries at $r = \infty$ and $r = 0$ when we consider the dynamics of the quark and antiquark. However, the situation would depend on the quantity of the corresponding field theory as shown below. Here two types of these wall are shown in Fig. 3. They depart from the common position with increasing b_0 for $C \neq 0$. Furthermore, the role of the wall is altered for the glueball or closed string state. This point is explained more in the next subsection.

B. Two boundaries

In performing the analysis in the present model, we must notice the point discussed in [9] that the bulk metric given here has two boundaries in the confinement region (A) shown in Fig. 1, $\lambda < 0$ and $0 \leq b_0 < r_0$. The two boundaries are found at $r = \infty$ (UV side) and $r = 0$ (IR side); however, there is no horizon between them. The reason why the horizon is absent is understood as follows. Each boundary is described by AdS_4, and its boundary is connected to the one of the other AdS_4. In this sense, these two boundaries are connected on their boundaries. It is an interesting problem to see how the two boundary theories are connected at their boundary. It would be reflected in the bulk, so we could resolve this point from the holographic approach, however it is postponed to concentrate on this point and to get a deeper understanding. Our purpose is to study the role of the dark radiation in the theory on the UV boundary. As for the IR boundary, we only give understandable few comments.

The holographic situation for these theories on the two boundaries depends on the parameter b_0 as explained below according to the horizontal axis b_0 in Fig. 3.

$b_0 = 0$.—As discussed in [9], in the case of $b_0 = 0$ and $\lambda < 0$, the bulk can be separated into two regions by a border called the domain wall, which is set at $r = r_0$. Then the field theory on each boundary is obtained from each bulk separated by this wall. Actually, in the present case, we find that the metrics are symmetric around $r = r_0$ under the transformation $r \to z = R^2/r$. Then we will find the same boundary four-dimensional theory. In other words, we could observe the same dynamical properties of the two field theories at $r = \infty$ and $z = 0$.

$0 < b_0 \leq r_0$.—In this region, the two theories show different properties from each other when the dark radiation C is added. In fact, in this case, we find different boundary metric, $g_0 \neq \hat{g}_0$, where g_0 ($\hat{g}_0$) denotes the metric on the boundary $r = \infty$ ($r = 0$), at the two boundaries. As a result, the energy momentum tensors are also different in each boundary as shown below. The point, we should notice, is that the metric at $r = 0$, $\hat{g}_0$, depends on b_0. Then the theories become asymmetric due to the dark radiation. On this point, we give a brief comment below.

(i) *For $r = \infty$*: The boundary metric g_0 is not altered by b_0 and is given as

$$ds^2 = -dt^2 + a_0^2(t)\gamma_{i,j}dx^i dx^j. \tag{2.19}$$

We notice here that the above metric depends only on λ, but it does not include the dark radiation C or b_0. This point is important. The dark radiation is instead observed as a perfect fluid of the gauge fields as seen in the energy momentum tensor $\langle T_{\mu\nu} \rangle$ [7].

The role of this fluid is to screen the confining force between colored charges. However, the confining force is overwhelming in the region $0 < b_0 \leq r_0$, where quark confinement is observed.

(ii) *For $r = 0$*: On the other hand, at $r = 0$, the metric $\hat{g}_0$ is deformed by the dark radiation b_0. It is given as follows [9]:

$$ds^2 = -\alpha_1 dt^2 + \alpha_2 a_0^2(t)\gamma_{i,j}dx^i dx^j. \tag{2.20}$$

$$\alpha_1 = \frac{(r_0^4 - b_0^4)^2}{(r_0{}^4 + b_0^4)r_0^4}, \qquad \alpha_2 = \frac{r_0{}^4 + b_0^4}{r_0^4}. \tag{2.21}$$

[3]Notice that we set $r_0 = R = 1$ in Fig. 2.

The tt component of this metric becomes zero at the critical point, $b_0 = r_0$. Then the event horizon appears. As for the energy momentum tensor $\langle T^{\rm IR}_{\mu\nu}\rangle$ on the boundary $r = 0$, which is given in [9], the perfect fluid part disappears.

This fact implies that the dark radiation works as a four-dimensional matter which couples to the gravity to reform the four-dimensional metric $\hat{g}_{(0)\mu\nu}$. Then the bulk would be dual to the pure SYM living in this deformed FRW space-time.

$r_0 < b_0$.—In the region of $r_0 < b_0$, the IR boundary hides behind the horizon, which appears at r_H for $r_0 < b_0$. Then we consider the region from a horizon r_H to $r = \infty$. In this case, the bulk is simply dual only to the theory at the boundary $r = \infty$. The theory is in the deconfinement phase with finite temperature. So we expect dynamical properties which are similar to the case of AdS_5-Schwartzschild bulk. However, as shown in Fig. 3, the domain wall for the entanglement entropy appears above the horizon. So we expect a slightly different thermodynamic properties in the present case compared to the one of AdS_5-Schwartzschild finite temperature theory.

In the following, we study the phase transition property through glueball spectra and entanglement entropy. After the transition to the deconfinement phase at $b_0 > r_0$, the theory we consider is restricted to the one at the boundary $r = \infty$. Then the glueball mass and entanglement entropy are observed from the UV boundary theory.

III. GLUEBALLS FROM BULK FIELD FLUCTUATIONS

In the confinement phase, $0 \le b_0 < r_0$, we could expect the existence of a glueball state in the dual theory. It is studied by solving the equation of motion of the field fluctuations in the bulk [22–30]. This is performed here by separating to two cases of the parameter b_0.

A. $b_0 = 0$ case

In this case, $C = 0$, then the corresponding glueball state is studied by solving the field equation of the quantum fluctuation of the bulk fields in the following background,

$$\begin{aligned} ds^2_{10} &= ds^2_5 + R^2 d\Omega^2_5 \\ ds^2_5 &= \frac{r^2}{R^2}\left(1+\frac{r_0^2}{r^2}\right)^2 \tilde{g}_{\mu\nu}dx^\mu dx^\nu + \frac{R^2}{r^2}dr^2 \\ \tilde{g}_{\mu\nu}dx^\mu dx^\nu &= (-dt^2 + a_0^2(t)\gamma_{ij}(x)dx^i dx^j). \end{aligned} \tag{3.1}$$

Graviton 2^{++}: As for the glueball spectrum, many attempts have been made by solving the linearized field equations of bulk field fluctuations in various background configurations. Here we consider the field equation of the traceless and transverse component of the metric fluctuation, which is denoted by h_{ij}. Its linearized equation is given in the Einstein frame metric as

$$\frac{1}{\sqrt{-g}}\partial_M(\sqrt{-g}g^{MN}\partial_N h_{ij}) = 0, \tag{3.2}$$

where we assumed as $h_{ij} = h_{ij}(x^0, x^i, r)$, then M, N are the five dimensional $((x^0, x^i, r))$ suffices.[4] This equation is equivalent to the massless scalar field equation. As shown in [29], this equation is common to $2^{++}, 1^{++}$ and the one of the nonactive[5] dilaton 0^{++} [31], which are dual to the glueball of $F_{\mu\nu}F^{\mu\nu}$. While it is usually used to derive the type IIA theory, the NS-NS part is common with the one of the type IIB theory. Then the masses of these three spin states degenerate.

By setting as $h_{ij} = p_{ij}\chi(x^\mu)\phi(r)$,[6] we impose for the four-dimensional part of the wave function, $\chi(x^\mu)$, the following eigenvalue equation,

$$\frac{1}{\sqrt{\tilde{g}_4}}\partial_\mu\sqrt{\tilde{g}_4}\tilde{g}^{\mu\nu}\partial_\nu\chi(x^\mu) = m^2\chi(x^\mu), \tag{3.3}$$

where $\tilde{g}_4 = -\det\tilde{g}_{\mu\nu}$. Then, we get for $\phi(r)$ the following equation:

$$\partial_r^2\phi + g_2(r)\partial_r\phi + \left(\frac{R}{r}\right)^4\frac{m^2}{A^2}\phi = 0, \tag{3.4}$$

$$g_2(r) = \partial_r(\log[(r/R)^5A^4]), \tag{3.5}$$

$$A(r) = 1 + \left(\frac{r_0}{r}\right)^2. \tag{3.6}$$

When Eq. (3.3) is regarded as the one for the free field in AdS_4 space-time, the eigenvalue of m^2 has been obtained as

$$m^2 = |\lambda|n(n+3), \tag{3.7}$$

for scalar ($n \ge 0$) in [32] and for spin two tensor ($n \ge 1$) in [33]. In the following, we could obtain the mass spectra of (3.7) for the glueball of 2^{++} in AdS_4. This fact implies the correctness of the holographic approach also to the theory living in AdS_4.

General solution.—In the present case, we can solve analytically the equation (3.4). Changing r to a dimensionless variable $x = r/r_0$, the above equations are rewritten as

$$\partial_x^2\phi + g_2(x)\partial_x\phi + \frac{\bar{m}^2}{x^4A^2(x)}\phi = 0, \tag{3.8}$$

[4]In the string frame metric case, this equation is written as $\frac{1}{\sqrt{-g}}\partial_M(\sqrt{-g}e^{-2\Phi}g^{MN}\partial_N h_{ij}) = 0$ as given in [23].

[5]Here, "active" means that the dilaton background solution is nontrivial as in the present case.

[6]p_{ij} denotes projection operator onto the traceless and transverse components.

$$g_2(r) = \frac{1}{x}\left(5 - \frac{8}{x^2 A(x)}\right), \tag{3.9}$$

$$A(x) = 1 + \left(\frac{1}{x^2}\right), \tag{3.10}$$

where $\bar{m} = R^2 m/r_0$. Equation (3.8) has two regular singularity at $x = 0$ and $x = \infty$. We solve this equation as follows. First, by setting the following form for ϕ,

$$\phi = A^a x^b P(x), \tag{3.11}$$

it is possible to write the equation for $P(x)$ as follows,

$$y(1-y)\partial_y^2 P + (\gamma - [\alpha + \beta + 1]y)\partial_x P - \alpha\beta P = 0, \tag{3.12}$$

where $y = -x^2$, and

$$\alpha = \frac{b}{2}, \qquad \beta = 2 + \frac{b}{2}, \qquad \gamma = b - 2a - 1. \tag{3.13}$$

As for a and b, we have four sets of solutions,

(i) $a = \frac{1}{2}(-3 - \sqrt{9 + \bar{m}^2})$, $b = 2a$,
(ii) $a = \frac{1}{2}(-3 - \sqrt{9 + \bar{m}^2})$, $b = 2a + 4$,
(iii) $a = \frac{1}{2}(-3 + \sqrt{9 + \bar{m}^2})$, $b = 2a$,
(iv) $a = \frac{1}{2}(-3 + \sqrt{9 + \bar{m}^2})$, $b = 2a + 4$.

The solution of (3.12) is given by Gauss's hypergeometric function as

$$P(y) = F(\alpha, \beta, \gamma; y), \tag{3.14}$$

and its behavior is well known. So we obtain the solution in the four forms of hyper-geometric function. Among them, we find that the solution (ii) and (iv) satisfy (3.8). Then the other two, (i) and (iii), are not the solution. Furthermore, we can show that the solution (ii) (denoted by ϕ_2) is equivalent to the one of (iv), then we get only one solution, ϕ_2, at this stage.

The other independent solution of (3.8) is given as

$$\phi_5 = Q(x)\phi_2(x), \tag{3.15}$$

then from (3.4), we obtain the equation of $Q(x)$ as

$$\partial_x^2 Q + (g_2(x)\phi_2 + 2\partial_x\phi_2)\partial_x Q = 0. \tag{3.16}$$

Dividing this equation by $\phi_2 \partial_x C$, we find

$$\log(\phi_2^2 \partial_x Q) = -\int g_2 dx. \tag{3.17}$$

This is solved as

$$\partial_x Q = \frac{\bar{q}_0}{\phi_2^2}\frac{x^3}{(1+x^2)^4}, \tag{3.18}$$

where $\bar{q}_0$ is an integral constant. Finally, we get

$$Q = \int dx \frac{\bar{q}_0}{\phi_2^2}\frac{x^3}{(1+x^2)^4}. \tag{3.19}$$

Here it is possible to add an arbitrary constant to the right-hand side of (3.19). However, it is not necessary since it is absorbed into the coefficient of ϕ_2 of the general solution. It is given as follows,

$$\phi = \alpha_2\phi_2 + \alpha_5\phi_5, \tag{3.20}$$

where α_2 and α_5 are constants. Further, we consider that $\bar{q}_0$ is absorbed into α_5 hereafter. They are determined by the boundary conditions on the two boundaries, $r = \infty$ and $r = 0$, as follows.

1. Glueball (normalizable) solution

In the limit of $r \to 0$, the above solutions are expanded as

$$\phi_2 = x^4\left(1 - \frac{32 + \bar{m}^2}{12}x^2 + O(x^4)\right) \to 0, \tag{3.21}$$

$$\phi_5 = -\frac{1}{4}\left(1 + \frac{\bar{m}^2}{4}x^2 + (q_4 + q_{4L}\ln x)x^4 + \cdots\right) \to \text{const.}$$

$$q_4 = -\frac{(8 + \bar{m}^2)(32 + \bar{m}^2)}{36}, \tag{3.23}$$

where q_{4L} is a constant. From (3.22), we find that ϕ_5 is non-normalizable since ϕ_5 is a constant at $r = 0$. This is understood as

$$\int dr\sqrt{g_{(5)}}|\phi_5|^2 \sim \int_{r\to 0} dr \frac{1}{r^3}|\phi_5|^2, \tag{3.24}$$

where the factor $1/r^3$ appears from $\sqrt{g_{(5)}}$ near $r = 0$ in the integral measure of the wave function. On the other hand, we find

$$\phi_2 \to \text{const} \tag{3.25}$$

in the limit of $r \to \infty$. This implies that this wave function includes the source of the field operators of the theory on the boundary $r = \infty$. The normalizable modes are also found for special values of m^2 given below. In this case, it behaves as

$$\phi_2 \to \frac{p_4}{x^4} + \cdots \tag{3.26}$$

with a constant p_4, thus the wave function ϕ_2 is normalizable.

Then we take $\phi = \phi_2$ as the wave function for the glueball, and we find that this solution is actually normalizable under the condition,

$$\sqrt{9+\tilde{m}^2} = 5 + 2n, \qquad n = 0, 1, 2, \ldots. \tag{3.27}$$

Thus we get the following mass spectra for the glueball considered here,

$$m^2 = 4(n+1)(n+4)\frac{r_0^2}{R^4} = |\lambda|(n+1)(n+4), \quad n = 0, 1, 2, \ldots. \tag{3.28}$$

This resulting formula is compared with the above formula (3.7). This coincides with the case of spin two tensor.[7] Namely, the lowest glueball mass is $m_0 = 2\sqrt{\lambda}$, which is also obtained here by the WKB approximation with high accuracy as shown below.

The analysis for the glueball mass given above is performed for the theory on the boundary $r = \infty$. In the present case of $b_0 = 0$, it is parallel to perform the same analysis for the theory at the boundary $r = 0$. The only thing we should do is to change the variable r to $z = r_0^2/r$, then we will find the same mass eigenvalues also in the theory at $z = \infty$. When the dark radiation is added, the symmetric situation is broken and the analysis becomes complicated as shown below.

B. $0 \le b_0 < r_0$ case : WKB approximation

When the finite value of C is introduced, it is impossible to solve analytically the equation of motion for the fluctuation mode of the bulk fields. So we consider here an alternative method to find the glueball spectra. The most popular and convenient one is the WKB method which has been used by many people [21,23–29].

$b_0 = 0$ *case.*—First, we perform this method to obtain the mass for the case of $C = 0$, then its results are compared with the one given in the previous section to assure that this approximation is good.

The equation (3.4) has two regular singularities at $r = 0, \infty$. Here, we try to find the eigenfunctions in the region of $0 \le r \le \infty$ through WKB approximation [23,26].

By factorizing ϕ as

$$\phi = e^{-\frac{1}{2}\int dr g_2(r)} f(r), \tag{3.29}$$

Eq. (3.4) is rewritten as

$$-\partial_r^2 f + V(r) f = 0, \qquad V = \frac{1}{4}g_2^2 + \frac{1}{2}\partial_r g_2 - \frac{m^2}{A^2}\left(\frac{R}{r}\right)^4. \tag{3.30}$$

This is equivalent to the one dimensional Schrödinger equation with the potential V and the zero energy eigenvalue. For an appropriate mass m, we can see that V has two turning points, r_1 and $r_2 (> r_1)$, to give [23]

$$\int_{r_1}^{r_2} \sqrt{-V} dr = \left(n + \frac{1}{2}\right)\pi \tag{3.31}$$

with an integer n. From this equation we obtain the discrete glueball mass m_n, where n denotes the node number of the eigenfunction. The potential for the zero node is shown in the Fig. 4. In this case, we have $\int_{r_1}^{r_2} \sqrt{-V} dr = \pi/2$ and the lowest mass with 4 percent numerical error compared to the correct eigenvalue obtained through an analytical solution given above.

$0 < b_0 < r_0$ *case.*—According to the procedure given above, we find the following equations for this case for glueball of 2^{++}. By setting as $h_{ij} = p_{ij}\chi(x^\mu)\phi(t, r)$, where $\chi(x^\mu)$ is assume to be satisfied (3.3) and $\phi(r)$ is replaced by $\phi(a_0(t), r)$ since the coefficients of the equation are written by using $a_0(t)$. Then, we get for $\phi(a_0(t), r)$ the following equations:

$$\partial_r^2\phi + \bar{g}_2(r)\partial_r\phi + \left(\frac{R}{r}\right)^4 \frac{m^2}{\bar{A}^2}\phi = J, \tag{3.32}$$

$$\bar{g}_2(r) = \partial_r(\log[(r/R)^5 \bar{n}\bar{A}^3]), \tag{3.33}$$

$$J = -\left(\frac{R}{r}\right)^4 \frac{\phi}{\chi\bar{A}^2}\left(\partial_t^2 + 3\frac{\dot{a}_0}{a_0}\partial_t\right)\chi + \left(\frac{R}{r}\right)^4 \frac{1}{\chi\bar{n}^2}\left(\partial_t^2 + 3\frac{\dot{a}_0}{a_0}\partial_t\right)(\chi\phi) - \left(\frac{R}{r}\right)^4 \frac{1}{\chi}\left(\frac{\partial_t(\bar{n})}{\bar{n}^3} - 3\frac{\partial_t(\bar{A})}{\bar{A}}\right)\partial_t(\chi\phi). \tag{3.34}$$

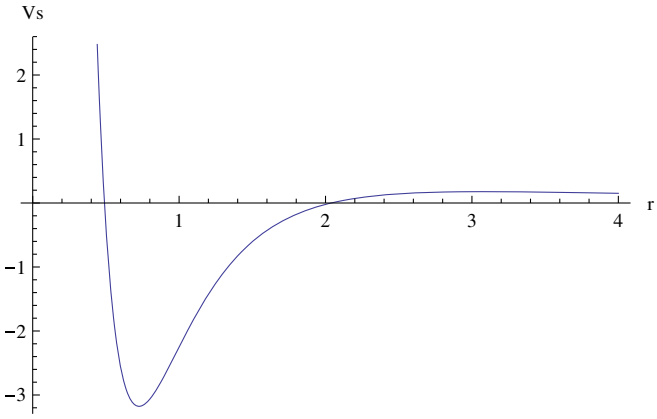

FIG. 4 (color online). The Schrödinger potentials $V(r)$ for $r_0 = R = 1$ and $|\lambda| = 4$ is shown for the graviton with $m = 2\sqrt{|\lambda|} = 4.0$, $r_1 = 0.4903$ and $r_2 = 2.0395$.

[7] In order to reproduce masses of the candidate for the tensor glueballs f_2 (1270 and 1525 MeV), we need $\sqrt{|\lambda|} = 0.71 \sim 0.84$ GeV. However, it would be difficult to find a realistic situation for these kinds of analyses in our world. So we postpone performing an estimation of this kind until a future paper.

The left-hand side of (3.32) has a similar form to (3.8), so we expect a stable glueball state. However, the term on the right-hand side, J, arises because of nonzero C. In spite of its complicated form, J is simplified when $\partial_t(a_0(t)) = \dot{a}_0$ is neglected according to our approximation adopted above. In this case, we find

$$J = \left(\frac{R}{r}\right)^4 \left(\frac{1}{\bar{A}^2} - \frac{1}{\bar{n}^2}\right)\Omega^2\phi, \tag{3.35}$$

where

$$-\Omega^2 = \frac{\partial_t^2\chi}{\chi}. \tag{3.36}$$

Furthermore, we simplify the situation so that the derivative with respect to the spacial coordinate for χ can be neglected. In this approximation, the WKB approximation would be useful especially for the ground state. Then we may set

$$\Omega^2 = m^2, \tag{3.37}$$

and we obtain

$$\partial_r^2\phi + \bar{g}_2(r)\partial_r\phi + \left(\frac{R}{r}\right)^4 \frac{m^2}{\bar{n}^2}\phi = 0. \tag{3.38}$$

Notice that the last term of the left-hand side is changed from $\bar{A}$ to $\bar{n}$. This point is the main and important difference from the case of $C = 0$. Due to this replacement, we find the glueball mass decreases with C and it tends to zero at the transition point $\tilde{c}_0^{1/4} = r_0/R$, where confinement is lost from. Of course, this equation is reduced to (3.8) for $C = 0$.

Equation (3.38) has two regular singularities at $r = 0, \infty$. Then, we perform the analysis through WKB approximation in the region of $0 \le r \le \infty$. By factorizing ϕ as

$$\phi = e^{-\frac{1}{2}\int dr \bar{g}_2(r)} f(r), \tag{3.39}$$

Eq. (3.4) is rewritten as

$$-\partial_r^2 f + \bar{V}(r) f = 0, \qquad \bar{V} = \frac{1}{4}\bar{g}_2^2 + \frac{1}{2}\partial_r\bar{g}_2 - \frac{m^2}{\bar{n}^2}\left(\frac{R}{r}\right)^4. \tag{3.40}$$

As shown above for $C = 0$ case, for an appropriate mass m, we can see that $\bar{V}$ has two turning points, r_1 and $r_2 (> r_1)$, which give

$$\int_{r_1}^{r_2} \sqrt{-\bar{V}}\, dr = \left(n + \frac{1}{2}\right)\pi \tag{3.41}$$

with an integer n. We show the numerical results for the lowest mass eigenvalue of $n = 0$ to see the effect of the dark radiation C.

1. The results of numerical analysis for $n = 0$

The glueball mass m_g of the ground state is obtained by WKB method as mentioned above. More specifically, m_g is calculated using (3.40) and (3.41) with $n = 0$. Numerical value of m_g is plotted as a function of b_0 in Fig. 5. The results are well fitted by

$$m_g = \sqrt{15.97(1 - b_0^4)} \approx 4\sqrt{1 - b_0^4}. \tag{3.42}$$

As expected, m_g decreases and vanishes at the critical point $b_0 = 1$.

Finally, we give the following comments of WKB analysis given here.

(1) The dark radiation C is related to b_0 as

$$b_0^4 = CR^3/(4a_0^4). \tag{3.43}$$

In the present analysis, a_0 is assumed to be almost constant. And $\mu = 1/R$ is fixed to be 1 in the present subsection. So the variation of b_0 corresponds to the one of C, which corresponds to the dark radiation energy density.

(2) It should be worthwhile to mention that there exist solutions of (3.40) and (3.41) even above the critical point. For example, the lightest mass is given by $m_g = 0.031$ with $n = 3$ when $b_0 = 1.005$. However the two turning points of this mode are seen at $r_1 = 0.086$ and $r_2 = 0.252$, and $r_H = 0.100 > r_1$ so that r_1 is hidden behind the horizon. In general, all the wave functions corresponding to the glueball are not well defined in the region $r_H < r < \infty$ since the region of $r_H > r > 0$ is needed. In other word, these modes might be unstable and might be swallowed into the region $r < r_H$ in the final step. In this sense, they correspond to the quasinormal mode in [20].

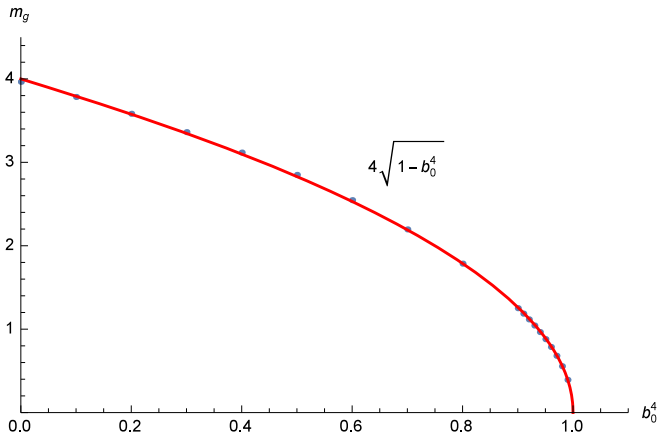

FIG. 5 (color online). The mass m_g is plotted against b_0^4. The mass m_g is defined by (3.40) and (3.41) with $n = 0$. There $r_0 = 1$, $R = 1$ and $\lambda = -4r_0^2/R^4 = -4$. The fitted curve is given by $m_g = 4\sqrt{1 - b_0^4}$.

(3) We should notice that the glueball mass studied above is the one for the theory at the boundary $r = \infty$. For the theory at $r = 0$, we could see the spectra by using the operator written by $\hat{g}_0$. This is abbreviated here and in the next section.

IV. GLUEBALLS AS ROTATING CLOSED STRING

In this section, we show the classical stable configuration of glueballs corresponding to the state of large quantum number. Then we support the above results for the C dependence of the glueball mass. The quantum fluctuations around the classical configuration can be neglected in this case. Flavored mesons are given by an open string whose two end points are on the D7 brane. On the other hand, the glueball with higher spin would be represented by a rotating closed string in the bulk. Such a rotating string is formulated according to [30,34–39] as follows.

In performing the analysis, we need only the five-dimensional bulk part of the metric, which is rewritten as

$$ds_5^2 = \frac{r^2}{R^2}(-\bar{n}^2 dt^2 + \bar{A}^2 ds_{(3)}^2) + \frac{R^2}{r^2} dr^2, \tag{4.1}$$

$$ds_{(3)}^2 = a_0^2(t)\gamma_{ij}(x)dx^i dx^j \tag{4.2}$$

$$= a_0^2(t)\left(\frac{dp^2}{1+p^2/\bar{r}^2} + p^2 d\Omega_{(2)}^2\right), \tag{4.3}$$

$$d\Omega_{(2)}^2 = d\bar{\theta}^2 + \sin^2\bar{\theta} d\bar{\phi}^2, \tag{4.4}$$

where $\Omega_{(2)}$ denotes the metric of S^2 with two angle coordinates $\bar{\theta}$ and $\bar{\phi}$, and

$$p = \frac{\bar{r}}{1 - \frac{\bar{r}^2}{4\bar{r}_0^2}}. \tag{4.5}$$

Here, we consider a closed string, which rotates around the podal axis of S^2 at a fixed value of $\bar{\theta}$.

Ansatz $p(r)$ and $\phi = \omega t$.—For simplicity, we consider the solution of the form given by $p(r)$ and $\phi = \omega t$. In this case, we have the induced metric for the string as

$$\mathcal{G}_{\tau\tau} = \frac{r^2}{R^2}\bar{A}^2(r)\left(-\frac{\bar{n}^2}{\bar{A}^2} + \omega^2 p^2 \sin^2\bar{\theta} a_0^2(t)\right), \tag{4.6}$$

$$\mathcal{G}_{\sigma\sigma} = \frac{R^2}{r^2} + \frac{r^2}{R^2}\bar{A}^2 \frac{p'^2}{1+p^2} a_0^2(t), \tag{4.7}$$

where ω is a constant and the prime denotes the derivative with respect to r. Then we have the following Nambu-Goto action for the closed string,

$$S_{\text{string}} = \int dt\mathcal{L} \tag{4.8}$$

$$= -\frac{1}{2\pi\alpha'}\int dt dr \frac{r^2}{R^2}\bar{A}^2 \sqrt{\left(\frac{\bar{n}^2}{\bar{A}^2} - \omega^2 p^2 \sin^2\bar{\theta} a_0^2(t)\right)\left(\frac{p'^2}{1+p^2} a_0^2(t) + \bar{A}^{-2}\left(\frac{R}{r}\right)^4\right)}. \tag{4.9}$$

From this, the spin J_s and the energy E_s of this string are formally given as

$$J_s = \frac{\partial\mathcal{L}}{\partial\omega} = \frac{1}{2\pi\alpha'}\int dr a_0^2 \frac{r^2}{R^2}\bar{A}^2 \omega p^2 \sin^2\bar{\theta} \times \sqrt{\frac{a_0^2(t)p'^2/(1+p^2) + \bar{A}^{-2}(\frac{R}{r})^4}{\bar{n}^2/\bar{A}^2 - \omega^2 p^2 \sin^2\bar{\theta} a_0^2(t)}}, \tag{4.10}$$

$$E_s = \omega\frac{\partial\mathcal{L}}{\partial\omega} - \mathcal{L} = \frac{1}{2\pi\alpha'}\int dr \frac{r^2}{R^2}\bar{n}^2 \sqrt{\frac{a_0^2(t)p'^2/(1+p^2) + \bar{A}^{-2}(\frac{R}{r})^4}{\bar{n}^2/\bar{A}^2 - \omega^2 p^2 \sin^2\bar{\theta} a_0^2(t)}}. \tag{4.11}$$

Solution

$b_0 = 0$ *case.*—In this case, we could find a solution of constant r as shown below. The Lagrangian is rewritten by supposing $r = r(p)$ as

$$\mathcal{L} = --\frac{1}{2\pi\alpha'}\int dp \frac{r^2}{R^2}\bar{A}^2 \times \sqrt{(1-\omega^2 p^2 \sin^2\bar{\theta} a_0^2(t))\left(\frac{a_0^2(t)}{1+p^2} + \frac{\dot{r}^2}{\bar{A}^2}\left(\frac{R}{r}\right)^4\right)}, \tag{4.12}$$

where $\dot{r} = \partial_p r$. Then imposing $r = \text{constant}$ ($\dot{r} = 0$), the equation of motion for r is given as

$$\partial_r\left(\frac{r^2}{R^2}\bar{A}^2\right) = 0. \tag{4.13}$$

The solution is found as

$$r = r_0. \tag{4.14}$$

The spin and the energy of this closed string configuration are given by using the above equations (4.10) and (4.11) as

$$J_s = \frac{1}{2\pi\alpha'}\frac{4a_0 l^2}{\omega}\frac{r_0^2}{R^2}\int_{-1/l}^{1/l} dp \frac{p^2}{\sqrt{(1+p^2)(1-l^2p^2)}}, \tag{4.15}$$

$$E_s = \frac{1}{2\pi\alpha'}4a_0\frac{r_0^2}{R^2}\int_{-1/l}^{1/l} dp \frac{1}{\sqrt{(1+p^2)(1-l^2p^2)}}, \tag{4.16}$$

where $l = \omega a_0 \sin\bar{\theta}$.

For small p, by approximating as $\sqrt{1+p^2} \sim 1$, we can estimate the above J_s and E_s as follows.

Substituting the above closed string solution, we find

$$J_s = \frac{Kl^2}{\omega}\int_{-1/l}^{1/l} dp \frac{p^2}{\sqrt{(1-l^2p^2)}} = \frac{K\pi}{2l\omega}, \tag{4.17}$$

$$E_s = K\int_{-1/l}^{1/l} dp \frac{1}{\sqrt{(1-l^2p^2)}} = \frac{K\pi}{l}. \tag{4.18}$$

$$K = \frac{1}{2\pi\alpha'}4a_0\frac{r_0^2}{R^2}. \tag{4.19}$$

Then we obtain

$$J_s = \alpha'_{\text{glueball}}E_s^2, \qquad \alpha'_{\text{glueball}} = \alpha'\frac{R^2}{r_0^2}\sin\bar{\theta}. \tag{4.20}$$

We could find the relation

$$\alpha'_{\text{glueball}} = \frac{1}{2}\alpha'_{\text{meson}}, \tag{4.21}$$

where α'_{meson} represents the slope parameter of the flavored mesons [30].

$b_0 \neq 0$ *case*.—In this case, there is no solution of constant r. And it is difficult to find any analytic solution of the equations of motion, then we perform numerical analysis in this case. For simplicity, we set as $r_0 = R = 1$ and $a_0 = 0.5$, then the equations are solved by varying the value of b_0 in the range of $0 \leq b_0 < 1$ to obtain the corresponding solution of $p(r)$. A typical configuration of the solution is shown in the Fig. 6 for $b_0 = 0.84$ and $\omega = 1.0$.

We notice that the center of the rotating string ($r_{D'}$) exists in the region of $0 < r < r_D$, where r_D denotes the domain wall given above and it separates the bulk to the two regions corresponding to the two theories which are living in the boundaries at $r = \infty$ and $r = 0$. $r_{D'}$ depends on ω. As $\omega \to 0$, then $r_{D'} \to r_D$. In the present case, the closed string solution appears in the region corresponding to the boundary $r = 0$. So we may consider that the glueball given here would be observed only in the theory at $r = 0$ boundary. However, as shown in the previous section, the wave function of the glueball extends in the both region even if the center of the function is at some point in the region of $0 < r < r_D$. In this sense, we could observe the glueball state in both boundaries.

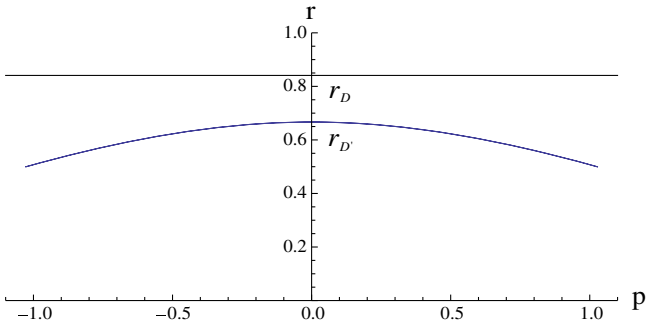

FIG. 6 (color online). The glueball solution $p(r)$ at $b_0 = 0.84$ and $\omega = 1.0$, where $r_D = 0.841$.

In the next, we show how this closed string configuration varies with b_0. Two quantities, (i) the position of its center ($r_{D'}$) and (ii) the length of glueball (L), are examined, and the $\Delta r/r_D = (r_D - r_{D'})/r_D$ and L are shown in the Fig. 7(left).

From this figure, we find that the string configuration shrinks to zero size when b_0 approaches to the critical value, $b_0 \to 1$. As for the point $r_{D'}$, it approaches to a point near the boundary $r = 0$ but it doesn't touch the boundary.

Further, by changing the value of ω, we can see the Regge behaviors

$$J_s = \alpha'_g E_s^2, \tag{4.22}$$

where α'_g depends on b_0. Further, α'_g is related to the string tension k as

$$\alpha'_g = 1/(8k). \tag{4.23}$$

The results for k are shown in the Fig. 7(right) for various b_0.

The string tension k comes to zero as $b_0 \to 1$. This is well described by the line

$$k = 0.11(1 - b_0^4). \tag{4.24}$$

For a state with spin one ($J = 1$), we have its mass as

$$m = 4\sqrt{1 - b_0^4}, \tag{4.25}$$

which is the same one obtained in the previous section from WKB approxiamtion.

Through the analyses of this and the previous section, we could see the existence of glueball state in the confinement region, $0 \leq b_0 \leq r_0$, and it disappears with its mass at the

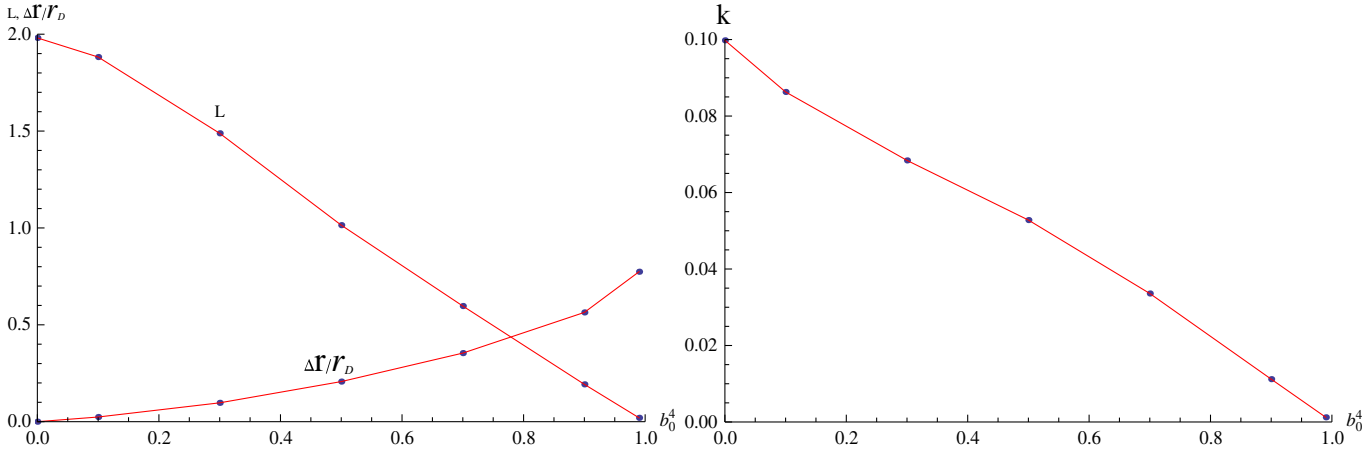

FIG. 7 (color online). Left: The string length L of the glueball and the ratio $\Delta r/r_D = (r_D - r_{D'})/r_D$ versus b_0^4 for $\omega = 1.0$. $L = \int \sqrt{1 + (dr/dp)^2}dp$. Right: The string tension k of the glueball versus b_0^4.

critical point $b_0 = r_0$. From this, we can say that we can set the order parameter of this transition as the tension of the QCD string.

V. ENTANGLEMENT ENTROPY AND DARK RADIATION

Here we study the entanglement entropy near the transition region to find an expected sign of the phase transition. As shown in [40] and [41], the holographic entanglement entropy is given by

$$S_{EE} = \frac{\mathrm{Area}(\gamma_A)}{4G_N^{(5)}}, \tag{5.1}$$

where γ_A denotes the minimal surface whose boundary is defined by ∂A and the surface is extended into the bulk. $G_N^{(5)} = G_N^{(10)}/(\pi^3 R^5)$ denotes the five-dimensional Newton constant reduced from the ten-dimensional one $G_N^{(10)}$.

Domain wall for minimal surface r_c: From (A4), the spatial part of the bulk metric is rewritten as

$$ds^2_{\mathrm{space}} = \frac{1}{R^2}\left(r^2 + 2r_0^2 + \frac{r_c^4}{r^2}\right)ds^2_{\mathrm{FRW}_3} + \frac{R^2}{r^2}dr^2 + R^2 d\Omega_5^2, \tag{5.2}$$

where

$$ds^2_{\mathrm{FRW}_3} = a_0^2(t)\gamma^2(dp^2 + p^2 d\Omega_2^2), \tag{5.3}$$

$$p = \frac{\bar{r}}{\bar{r}_0}, \qquad \gamma = 1/(1 - p^2/4), \tag{5.4}$$

and r_c is defined as

$$r_c \equiv (b_0^4 + r_0^4)^{1/4}. \tag{5.5}$$

Notice that, in this section, p in (5.4) is different from (4.5). As mentioned in Sec. II, the point $r = r_c$ is called the domain wall since the solution of the minimal surface cannot penetrate this point. Namely the solution is restricted to the region $r_c < r < \infty$ or $0 < r < r_c$.

As for the part of $0 < r < r_c$, the coordinate is rewritten in a similar form to the one of $r_c < r < \infty$ by the following change of the variable. Change r to z as

$$z = r_c^2/r, \tag{5.6}$$

then the spatial part of the bulk metric (5.2) becomes

$$ds^2_{\mathrm{space}} = \frac{1}{R^2}\left(z^2 + 2r_0^2 + \frac{r_c^4}{z^2}\right)ds^2_{\mathrm{FRW}_4} + \frac{R^2}{z^2}dz^2 + R^2 d\Omega_5^2. \tag{5.7}$$

It is obvious that the solution would be obtained in the side $z_c < z < \infty$ in the same form with the one given for $r_c < r < \infty$ by changing r to z. Thus it is convenient to use the transformation (5.6). In $b_0 < r_0$, there is a domain wall at $z = r_c$.

A. Minimal surface configuration

Here we consider an entangling surface at $z = 0$ as a ball with the radius p_0. Then the area of the minimal surface with this boundary is given by

$$\frac{S_{\mathrm{Area}}}{4\pi} = \int_0^{z(p=0)} dz\mathcal{L}(z), \tag{5.8}$$

where

$$\mathcal{L}(z) \equiv p(z)^2 B\sqrt{Bp'(z)^2 + \frac{R^2}{z^2}}, \tag{5.9}$$

and

$$B \equiv \frac{a_0^2\gamma^2}{R^2}\left(z^2+\frac{r_c^4}{z^2}+2r_0^2\right). \tag{5.10}$$

By solving the variational equations from (5.8), we can get the minimal surface $p(z)$. The numerical solutions for the confinement phase ($b_0 < r_0$) and deconfinement phase ($r_0 \le b_0$) are shown in Fig. 8, where p_0 denotes the ball radius on γ_A,

$$p_0 \equiv p(z=0) \le 2. \tag{5.11}$$

The upper bound comes from its definition.

In the confinement phase, the solutions for $p(r)$ at small r are obtained in the same form with the one given in the left-hand side of the Fig. 8 by replacing z by r.

On the other hand, in deconfinement phase, horizon ($z = z_h \equiv r_c^2/r_h$) appears in the small r side from the domain wall ($z = r_c$) as shown in the right-hand side of the Fig. 8. This relation is understood from

$$z_H^4 - r_c^4 = 2b_0^2 r_0^2\left(\frac{z_h}{r_c}\right)^4 \ge 0, \tag{5.12}$$

then the domain wall r_c is smaller than the horizon z_h. The solutions of small z side could not pass the domain wall, then they are away from the horizon. However, the solutions in the small r side, which are obtained by replacing z by r in the right of the Fig. 8, then the horizon is given by $r_H = r_c^2/z_H = 1.46$. Then the upper two solutions for $p_0 = 1.33$ and $p_0 = 1.99$ shown in the figure cross the horizon. When we reject such solutions as acausal, the upper bound (5.11) is modified by the value depending on b_0. In this sense, the phase transition is reflected in the theory at boundary $r = 0$.

In the next, we try to find the sign of the phase transition in the theory at $z = 0$. In this case, we use the bound (5.11) at any value of b_0.

B. Asymptotic solution for $p(z)$ and divergent terms

The solution $p(z)$ is expanded around $z = 0$ as

$$p = p_0 + p_2 z^2 + p_4 z^4 + p_{4L} z^4 \log z \ldots, \tag{5.13}$$

where $p_0 = p(z=0)$ and p_4 are arbitrary constants. p_2 is determined as

$$\begin{aligned} p_2 &= -\frac{(1-(p_0^2/4)^2)R^4}{2a_0^2 p_0 r_c^4}, \\ p_{4L} &= -\frac{(1-(p_0^2/4)^2)R^8\dot{a}_0^2}{4a_0^4 p_0 r_c^8}, \end{aligned} \tag{5.14}$$

where we used (2.6) with $k = -1$. When the time dependence of $\dot{a}_0(t)/a_0(t)$ is small ($\dot{a}_0 \sim 0$), $p_{4L} \sim 0$.

By using (5.13) and (5.14), the integrand (5.9) is expanded around $z = 0$ as

$$\mathcal{L}(z) = \frac{16a_0^2p_0^2r_c^4}{(p_0^2-4)^2R}\frac{1}{z^3} + \frac{64a_0^2p_0^2r_0^2-(p_0^2+4)^2}{2(p_0^2-4)^2R}\frac{1}{z} + \mathcal{O}(z). \tag{5.15}$$

Then, the area of the minimal surface of the region with radius $p = p_0$ is given by

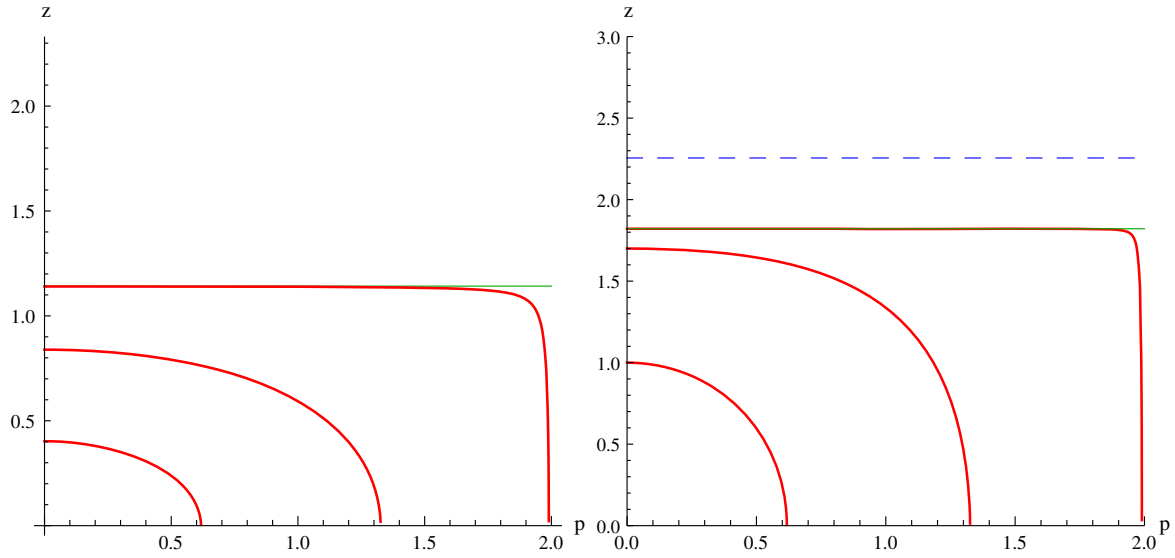

FIG. 8 (color online). *Left:* Embedded solutions for $p(z)$ for $p_0 = 0.62$, 1.33 and 1.99 with $r_0 = R = 1, a_0 = 0.5, b_0 = 0.18$. The green line is the domain wall $r_c = 1.14$. *Right:* Embedded solutions for $p(z)$ for $p_0 = 0.62$, 1.33 and $p_0 = 1.99$ with $r_0 = R = 1, a_0 = 0.5, b_0 = 2.5$. The green line is the domain wall $r_c = 1.82$ and the dashed blue line is the event horizon $z_H = 2.26$.

$$\frac{S_{\text{Area}}}{4\pi} = \int_{\epsilon}^{z(p=0)} dz\mathcal{L}(z) \tag{5.16}$$

$$= \frac{8a_0^2 r_c^4 p_0^2}{(p_0^2-4)^2 R}\frac{1}{\epsilon^2} - \frac{64a_0^2 p_0^2 r_0^2 - (p_0^2+4)^2 R^4}{2(p_0^2-4)^2 R} \times \log\left(\frac{\epsilon}{p_0}\right) + S_{\text{finite}}, \tag{5.17}$$

where the first and second term is the UV ($\epsilon \to 0$) divergent terms, and S_{finite} is a finite terms for UV limit ($z = \epsilon \to 0$). Then, from (5.1) and the relation $R^4 = 4\pi g_s \alpha'^2 N$, the entanglement entropy becomes

$$S_{EE} = \gamma_1 \frac{\text{Area}(\partial A)}{4\pi\epsilon^2} + \gamma_2 \log\left(\frac{p_0}{\epsilon}\right)\ldots \tag{5.18}$$

$$\gamma_1 = \frac{N^2 r_c^4}{R^4}, \tag{5.19}$$

$$\gamma_2 = N^2\left(1 + \frac{\text{Area}(\partial A)}{4\pi}\left(\frac{\dot{a}_0}{a_0}\right)^2\right), \tag{5.20}$$

where $k_0 = p_0/(1-p_0^2/4)$ and $\text{Area}(\partial A)$ denote the proper area of the surface A which is defined as

$$\text{Area}(\partial A) = 4\pi k_0^2 a_0(t)^2. \tag{5.21}$$

The second term of (5.20) is the effect of the curvature of FRW_4 [42].

When the time dependence of $a_0(t)$ is small ($\dot{a}_0 \sim 0$), $\gamma_2 \sim N^2$, which is the degree of freedom in the dual field theory.

C. Behavior of the finite part S_{finite}

Next we observe the behavior of the finite part S_{finite} of the entanglement entropy. On the boundary $z = 0$, this quantity is calculated by using the common formula in all the range of b_0.

In the Fig. 9, S_{finite}/V is shown for $p_0 = 1.99, V = 2488, a_0 = 0.5, R = r_0 = 1$. Here, S_{finite} is normalized by the volume V of the sphere with radius $p = p_0$ in FRW_4 space (5.7). It is given as

$$V = a_0^3 \int_0^{p_0} \gamma^3 p^2 dp = \frac{1}{2}a_0^3\left(\frac{4p_0(4+p_0^2)}{(p_0^2-4)^2} + \log\frac{2-p_0}{2+p_0}\right). \tag{5.22}$$

From the figure, we can't see any abrupt change near the transition point. However, its b_0 dependence changes from the small to the large b_0. For small $\tilde{b}_0$ region,

$$S_{\text{finite}}/V = 0.97 b_0^4 + 4.01, \tag{5.23}$$

and large b_0 region.

$$S_{\text{finite}}/V = 2.05 b_0^3 + 0.32 b_0. \tag{5.24}$$

Here notice that we set $R = 1$ in the above formula. This implies that the increasing behaviour of the entropy in the two regions seems to be dominated by different dynamical origin in each region. The transition from the one at small b_0 to the larger one seems smooth. The values are obtained at $p_0 = 1.99$. This means the entanglement entropy is estimated for large volume limit. In this case, we would expect that the entanglement entropy approaches to the usual thermal entropy of the system when it has temperature. In the present case, the first term of (5.24) indicates $S \propto T^3$, the behavior of the thermal entropy with the temperature T.

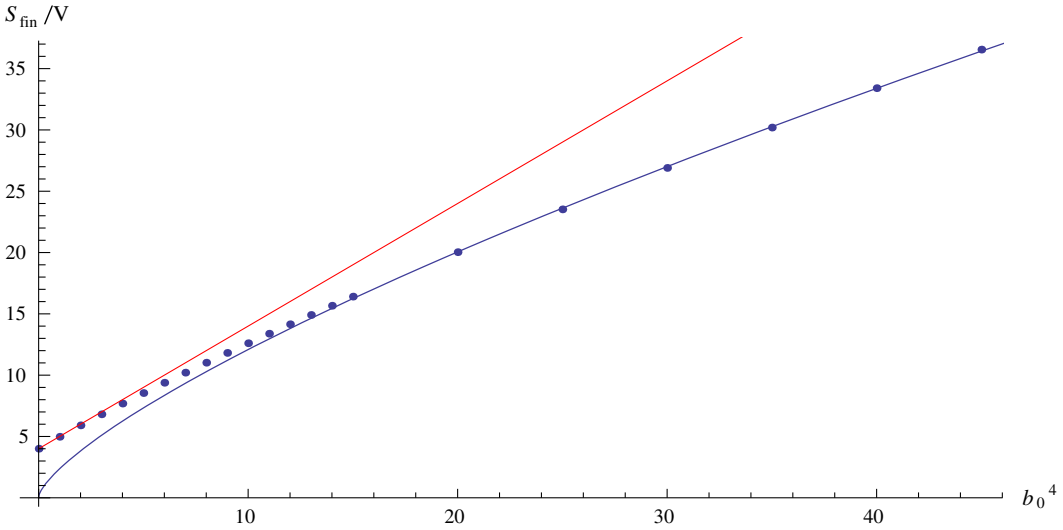

FIG. 9 (color online). A dotted line is S_{finite}/V with b_0^4 at $p_0 = 1.99, V = 2488, a_0 = 0.5, r_0 = R = 1$. S_{finite} can be fitted by $S_{\text{finite}}/V = 0.97 b_0^4 + 4.01$ at small b_0 region and $S_{\text{finite}}/V = 2.05 b_0^3 + 0.32 b_0$ at large b_0 region, respectively.

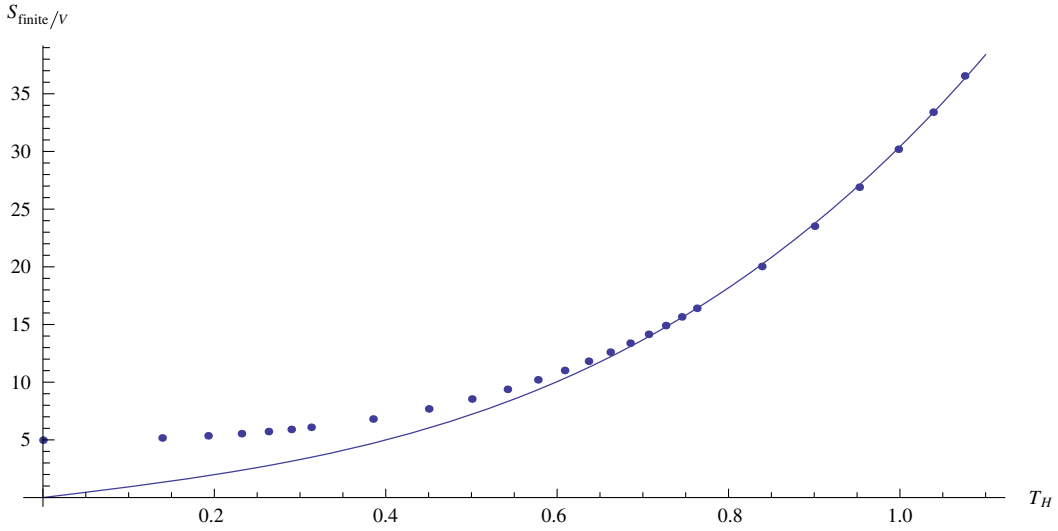

FIG. 10 (color online). A dotted line is S_{finite}/V with T_h at $p_0 = 1.99, a_0 = 0.5, V = 2488, R = r_0 = 1$. S_{finite} can be fitted by $S_{\text{finite}} = 20.4T_h^3 + 9.06T_h$ for large T_h.

Actually, in deconfinement phase ($b_0 \geq r_0$), the Hawking temperature T_h appears with the event horizon at r_H, and it is calculated as Appendix (B1). Then we plot T_h dependence of finite part of the entanglement entropy S_{finite} for $b_0^4 > 1$ in Fig. 10. As expected, we find the behavior, $S_{\text{finite}} \propto T_h^3$ for the region of large temperature as shown in [43]. This point is assured by the behavior of the thermal entropy which is shown in Appendix B.

In the confinement phase ($b_0 < r_0$), however, S_{finite} increases with b_0^4 as shown in Fig. 9. This behavior will be discussed in the future.

VI. SUMMARY AND DISCUSSION

We have examined the gravity dual of the SYM theory in the FRW type space-time, which is controlled by two essential ingredients, the four-dimensional cosmological constant λ and the dark radiation C. For negative λ and $C = 0$, the SYM theory is in the confinement phase. On the other hand, the theory is in the deconfinement phase with finite temperature for $\lambda = 0$ and finite C. This implies that the dark radiation works as a thermal bath of the SYM system. When both the negative λ and C are existing at the same time, they compete each other, and we can observe the phase transition from the confinement to the deconfinement phase when the value of C increases from very small value.

Here, through the glueball spectra and the entanglement entropy, we have studied how this phase transition is observed by varying the magnitude of C. As for the glueball, we could show the exact form of the glueball spectra in the case of $C = 0$ by solving the equation analytically, and we could assure that the result is consistent with the one of the free fields in the AdS_4 space-time. The latter was given in field theory many years ago [32,33].

When the dark radiation C is added in this system, it becomes difficult to obtain the analytical result. Then we adopted WKB approximation and examined the lowest glueball mass numerically, and we find that the mass decreases with increasing dark radiation in the region of confinement phase. Then, near the critical point, the mass of the glueball seems to be vanishing. This behavior is also observed by solving the classical closed string state in the bulk. This is corresponding to the high mass glueball state with higher spin. In this analysis, however, we must be careful in the region of small mass which is realized near the critical point since the quantum corrections would be important in this region. In any case, the glueball state disappears above the critical value of the dark radiation. Then the system moves to the high temperature deconfinement phase, where the temperature is given by the Hawking temperature whose value is determined by the dark radiation C.

In the analysis of the glueball, we give a comment related to the two boundaries which exist in the confinement region. The two theories on each boundary are symmetric at $C = 0$, and then the mass spectra are the same with each others. However, when the dark radiation is added, it works differently in the two boundaries. As a result, we find two different theories for $C \neq 0$. Here, we have examined the mass m, which is defined in the theory at the boundary $r = \infty$. It would be possible to see the mass defined on the boundary $r = 0$ by using $\hat{g}^{00}m^2$ and $z = r_0^2/r$. To study more on this point is postponed as a future work.

As for the entanglement entropy, its behavior is described in a symmetric form in both boundaries in the confinement phase. However, in the deconfinement phase or large C region, in the theory on the boundary $r = 0$, the size of the connected minimal surface is restricted by the value of C when the surface is restricted to the causal

region. In other words, the large-sized surface is disconnected since the small-sized part is cut off by the horizon.

So we have examined the entanglement entropy observed from $r = \infty$ boundary in order to find a sign of the phase transition near the critical point. While we could not find a clear transition sign at the critical point, we could observe thermal entropy for large volume area in the deconfinement phase. The entanglement entropy grows like T_H^3 at large T_H. On the other hand, in the confinement phase, the entanglement entropy increases with the dark radiation linearly. On this point, we will discuss in the future.

ACKNOWLEDGMENTS

The work of M. Ishihara was supported by the World Premier Researchã Institute Initiative, promoted by the Ministry of Education, Culture, Sports, Science, and Technology of Japan (MEXT). M. I. thanks the participants of the YIPQS workshops "Holographic Vistas on Gravity and Strings" for useful discussions.

APPENDIX A: BRIEF REVIEW OF THE MODEL

First, we briefly review our model [7–9]. We start from the ten-dimensional type IIB supergravity retaining the dilaton Φ, axion χ and selfdual five form field strength $F_{(5)}$,

$$S = \frac{1}{2\kappa^2}\int d^{10}x\sqrt{-g} \times \left(R - \frac{1}{2}(\partial\Phi)^2 + \frac{1}{2}e^{2\Phi}(\partial\chi)^2 - \frac{1}{4\cdot 5!}F_{(5)}^2\right), \quad \text{(A1)}$$

where other fields are neglected since we do not need them, and χ is Wick rotated [44]. Under the Freund-Rubin ansatz for $F_{(5)}$, $F_{\mu_1\ldots\mu_5} = -\sqrt{\Lambda}/2\epsilon_{\mu_1\ldots\mu_5}$ [45,46], and for the ten-dimensional metric as $M_5 \times S^5$,

$$ds_{10}^2 = g_{MN}dx^M dx^N + g_{ij}dx^i dx^j = g_{MN}dx^M dx^N + R^2 d\Omega_5^2,$$

we consider the solution. Here, the parameter is set as $(\mu =)1/R = \sqrt{\Lambda}/2$.

While the dilaton Φ and the axion χ play an important role when the bounadary of M_5 is given by Minkowski space-time [45–47], we neglect them here since we study the case of (A)dS$_4$ boundary. Then the equations of motion of noncompact five dimensional part M_5 are written as[8]

$$R_{MN} = -\Lambda g_{MN}. \quad \text{(A3)}$$

While this equation leads to the solution of AdS$_5$, there are various AdS$_5$ forms of the solutions which are discriminated by the geometry of their four-dimensional boundary as shown below.

1. Solution

A class of solutions of the above equation (A3) is obtained in the following form of metric [9],

$$ds_{10}^2 = \frac{r^2}{R^2}(-\bar{n}^2dt^2 + \bar{A}^2a_0^2(t)\gamma_{ij}(x)dx^i dx^j) + \frac{R^2}{r^2}dr^2 + R^2 d\Omega_5^2, \quad \text{(A4)}$$

where

$$\gamma_{ij}(x) = \delta_{ij}\left(1 + k\frac{\bar{r}^2}{4\bar{r_0}^2}\right)^{-2}, \qquad \bar{r}^2 = \sum_{i=1}^{3}(x^i)^2, \quad \text{(A5)}$$

and $k = \pm 1$, or 0. The arbitrary scale parameter $\bar{r_0}$ is set hereafter as $\bar{r_0} = 1$. For the undetermined noncompact five-dimensional part, the following equation is obtained from the tt and rr components of (A3) [11,12],

$$\left(\frac{\dot{a}_0}{a_0}\right)^2 + \frac{k}{a_0^2} = -\frac{\Lambda}{4}A^2 + \left(\frac{r}{R}A'\right)^2 + \frac{C}{a_0^4A^2}, \quad \text{(A6)}$$

where $\dot{a_0} = \partial a_0/\partial t$, $A' = \partial A/\partial r$, and

$$A = \frac{r}{R}\bar{A}, \qquad \frac{\partial_t(a_0(t)A)}{\dot{a}_0(t)} = \frac{r}{R}\bar{n}. \quad \text{(A7)}$$

The constant C is given as an integral constant in obtaining (A6), and we could understand that it corresponds to the thermal excitation of $\mathcal{N} = 4$ SYM theory for $a_0(t) = 1$, and it is called as dark radiation [11,12].

At this stage, two undetermined functions, $\bar{A}(r,t)$ and $a_0(t)$, are remained. However the equation to solve them is the Eq. (A6) only. Therefore, we could determine $a_0(t)$ by introducing the four-dimensional Friedmann equation, which is independent of (A3). However it should be realized on the boundary where various kinds of matter could be added in order to form the presumed FRW universe as in [9]

$$\left(\frac{\dot{a}_0}{a_0}\right)^2 + \frac{k}{a_0^2} = \frac{\Lambda_4}{3} + \frac{\kappa_4^2}{3}\left(\frac{\rho_m}{a_0^3} + \frac{\rho_r}{a_0^4} + \frac{\rho_u}{a_0^{3(1+u)}}\right) \equiv \lambda(t), \quad \text{(A8)}$$

where κ_4 (Λ_4) denotes the four-dimensional gravitational constant (cosmological constant). The quantities ρ_m and ρ_r denote the energy density of the nonrelativistic matter and

[8]The five-dimensional M_5 part of the solution is obtained by solving the following reduced Einstein frame five-dimensional action,

$$S = \frac{1}{2\kappa_5^2}\int d^5x\sqrt{-g}(R + 3\Lambda), \quad \text{(A2)}$$

which is written in the string frame and taking $\alpha' = g_s = 1$ and the opposite sign of the kinetic term of χ is due to the fact that the Euclidean version is considered here [44].

the radiation of four-dimensional theory, respectively. The most right-hand side expression $\lambda(t)$ in (A8) is given as a simple form of the most left-hand side of (A8) given by using $a_0(t)$. Then the remaining function $A(t,r)$ is obtained from (A6) in terms of $\lambda(t)$. The last term ρ_u in the middle of (A8) represents an unknown matter with the equation of state, $p_u = u\rho_u$, where p_u and ρ_u denote its pressure and energy density, respectively. It is important to be able to solve the bulk equation (A6) in this way by relating its left-hand side to the Friedmann equation defined on the boundary [9] since we could have a clear image for the solution.

Finally, the solution is obtained as

$$\bar{A} = \left(\left(1 - \frac{\lambda R^2}{4}\left(\frac{R}{r}\right)^2\right)^2 + \tilde{c}_0\left(\frac{R}{r}\right)^4\right)^{1/2}, \tag{A9}$$

$$\bar{n} = \frac{(1 - \frac{\lambda R^2}{4}(\frac{R}{r})^2)(1 - \frac{\lambda + \frac{a_0}{\dot{a}_0}\dot{\lambda}}{4\mu^2}(\frac{R}{r})^2) - \tilde{c}_0(\frac{R}{r})^4}{\sqrt{(1 - \frac{\lambda R^2}{4}(\frac{R}{r})^2)^2 + \tilde{c}_0(\frac{R}{r})^4}}, \tag{A10}$$

where

$$\tilde{c}_0 = CR^2/(4a_0^4). \tag{A11}$$

APPENDIX B: THERMAL ENTROPY

In the deconfinement phase, the horizon appears at $r = r_H = \sqrt{b_0^2 - r_0^2}$, then the Hawking temperature $T_H(b_0)$ in this case is obtained as

$$T_H(b_0) = \frac{r_H(1 + \frac{r_0^2 + b_0^2}{r_H^2})}{\pi R^2 \bar{A}(r_H)}, \tag{B1}$$

which approaches to T_H given by (2.7) for $r_0 \to 0$. Then the Euclidean action in this case is estimated as

$$\begin{aligned}\beta F = I &= \frac{1}{2\kappa_5^2}\int d^5x\sqrt{-g}(R + 3\Lambda) \\ &= -\frac{\Lambda}{2\kappa_5^2}\frac{V_3}{T_H(b_0)}\int_{r_H}^{\infty} dr\left(\frac{r}{R}\right)^3 \bar{n}\bar{A}^3,\end{aligned} \tag{B2}$$

$$V_3 = 4\pi a_0^3 \int dp \frac{p^2}{\sqrt{1+p^2}}, \tag{B3}$$

where V_3 denotes the three dimensional volume of the thermal system.

Then the regularized free energy F is obtained as follows,

$$\int_{r_H}^{\infty} dr\left(\frac{r}{R}\right)^3 \bar{n}\bar{A}^3 = ar_H^4 + br_H^2 + O(r_H^0), \tag{B4}$$

where the coefficients a, b are written by r_0 and R. Then we can see at large b_0

$$F \propto T_H^4, \quad \text{then } S \propto T_H^3 \tag{B5}$$

as in the case of $r_0 = 0$, namely in the Minkowski spacetime case.

APPENDIX C: DOMAIN WALL r_c FOR MINIMAL SURFACE

In Sec. V, the minimal surface is defined. It is obtained by finding the profile of the surface as a solution of the variational equation of the function (5.8), which is rewritten as

$$\frac{S_{\text{Area}}}{4\pi} = 2\int_0^{p(z=0)} dp\mathcal{L}(p), \tag{C1}$$

where

$$\begin{aligned}\mathcal{L}(p) &\equiv p^2 B\sqrt{B + \frac{R^2 z'(p)^2}{z^2}}, \\ z'(p) &= \frac{\partial z}{\partial p}\end{aligned} \tag{C2}$$

and

$$B \equiv \frac{a_0^2\gamma^2(p)}{R^2}\left(z^2 + \frac{r_c^4}{z^2} + 2r_0^2\right). \tag{C3}$$

Here $p(0) \equiv p_0 < 2$, and then we expect the maximum of $z(p)(\equiv z_c)$ is realized at the limit of $p_0 \to 2$. As a result, the minimal surface could not penetrate z_c, which is obtained as follows.

At the limit of $p_0 \to 2$, S_{Area} can be approximated as

$$\begin{aligned}\frac{S_{\text{Area}}}{2\pi} &= \int_{0,z=z_c,\partial z/\partial p=0}^{p_0} dp p^2 B^{3/2} \\ &\quad + \int_{0,p=p_0,\partial p/\partial z=0}^{z_c} dz p^2 B\frac{R^2}{z}\end{aligned} \tag{C4}$$

$$\begin{aligned}&= \int_0^{p_0} dp p^2\left(\frac{a_0^2\gamma^2}{R^2}f(z_c)\right)^{3/2} \\ &\quad + \int_0^{z_c} dz p_0^2 a_0^2\gamma^2(p_0)g(z),\end{aligned} \tag{C5}$$

where

$$f(z_c) = z_c^2 + \frac{r_c^4}{z_c^2} + 2r_0^2, \tag{C6}$$

$$g(z) = z + \frac{r_c^4}{z^3} + 2\frac{r_0^2}{z}. \tag{C7}$$

Here we notice that the first term is dominant for $p_0 \to 2$ since it increases with the volume of A. On the other hand, the second term increases with the surface of A. We could see that the first term has its minimum at $z_c = r_c$ from the form of $f(z_c)$ given above. Then we could understand that the value r_c corresponds to the domain wall for the minimal surface.

Another point to be noticed is that r_c is larger than the point of horizon r_H in the deconfinement phase. Then the minimal surface bounded at $r = 0$ could penetrate the horizon since it could stretch up to the domain wall $r_c (> r_H)$. On the other hand, the surface bounded at $r = \infty$ could not touch r_H since it starts from the opposite side.

[1] J. M. Maldacena, Adv. Theor. Math. Phys. **2**, 231 (1998); Int. J. Theor. Phys. **38**, 1113 (1999).
[2] S. S. Gubser, I. R. Klebanov, and A. M. Polyakov, Phys. Lett. B **428**, 105 (1998).
[3] E. Witten, Adv. Theor. Math. Phys. **2**, 253 (1998).
[4] T. Hirayama, J. High Energy Phys. 06 (2006) 013.
[5] K. Ghoroku, M. Ishihara, and A. Nakamura, Phys. Rev. D **74**, 124020 (2006).
[6] K. Ghoroku, M. Ishihara, and A. Nakamura, Phys. Rev. D **75**, 046005 (2007).
[7] J. Erdmenger, K. Ghoroku, and R. Meyer, Phys. Rev. D **84**, 026004 (2011).
[8] J. Erdmenger, K. Ghoroku, R. Meyer, and I. Papadimitriou, Fortschr. Phys. **60**, 991 (2012).
[9] K. Ghoroku and A. Nakamura, Phys. Rev. D **87**, 063507 (2013).
[10] K. Ghoroku, M. Ishihara, and A. Nakamura, Phys. Rev. D **89**, 066009 (2014).
[11] P. Binetruy, C. Deffayet, U. Ellwanger, and D. Langlois, Phys. Lett. B **477**, 285 (2000).
[12] D. Langlois, arXiv:hep-th/0005025.
[13] T. Shiromizu, K. Maeda, and M. Sasaki, Phys. Rev. D **62**, 024012 (2000).
[14] M. Sasaki, T. Shiromizu, and K. Maeda, Phys. Rev. D **62**, 024008 (2000); K. Maeda, S. Mizuno, and T. Torii, Phys. Rev. D **68**, 024033 (2003).
[15] A. Karch and L. Randall, J. High Energy Phys. 05 (2001) 008; 06 (2001) 063.
[16] J. Maldacena and L. Maoz, J. High Energy Phys. 02 (2004) 053.
[17] M. Kruczenski, D. Mateos, R. C. Myers, and D. J. Winters, J. High Energy Phys. 07 (2003) 049.
[18] N. Evans, J. French, K. Jensen, and E. Threlfall, Phys. Rev. D **81**, 066004 (2010).
[19] B. Gwak, M. Kim, B.-H. Lee, Y. Seo, and S.-J. Sin, arXiv:1105.2872.
[20] N. Evans and E. Threlfall, Phys. Rev. D **78**, 105020 (2008).
[21] K. Ghoroku, K. Kubo, T. Taminato, and F. Toyoda, J. High Energy Phys. 04 (2012) 087; arXiv:1111.7032.
[22] H. Ooguri, H. Robins, and J. Tannenhauser, Phys. Lett. B **437**, 77 (1998).
[23] J. A. Minahan, J. High Energy Phys. 01 (1999) 020.
[24] N. R. Constable and R. C. Myers, J. High Energy Phys. 11 (1999) 020.
[25] N. R. Constable and R. C. Myers, J. High Energy Phys. 10 (1999) 037.
[26] C. Csaki, H. Ooguri, Y. Oz, and J. Terning, J. High Energy Phys. 01 (1999) 017.
[27] E. Caceres and R. Hernandez, Phys. Lett. B **504**, 64 (2001).
[28] J. M. Pons, J. G. Russo, and P. Talavera, Nucl. Phys. **B700**, 71 (2004).
[29] R. C. Brower, S. D. Mathur, and C.-I. Tan, Nucl. Phys. **B587**, 249 (2000).
[30] K. Ghoroku, T. Taminato, and F. Toyoda, J. High Energy Phys. 05 (2011) 006.
[31] M. Giovannini, Phys. Rev. D **64**, 064023 (2001).
[32] S. J. Avis, C. J. Isham, and D. Storey, Phys. Rev. D **18**, 3565 (1978).
[33] C. Fronsdal, Phys. Rev. D **20**, 848 (1979).
[34] L. A. Pando Zayas, J. Sonnenschein, and D. Vaman, Nucl. Phys. **B682**, 3 (2004).
[35] F. Bigazzi, A. L. Cotrone, L. Martucci, and L. A. Pando Zayas, Phys. Rev. D **71**, 066002 (2005).
[36] M. Kruczenski, L. A. Pando Zayas, J. Sonnenschein, and D. Vaman, J. High Energy Phys. 06 (2005) 046.
[37] A. Paredes and P. Talavera, Nucl. Phys. **B713**, 438 (2005).
[38] I. Kirsch and D. Vaman, Phys. Rev. D **72**, 026007 (2005).
[39] M. Huang, Q.-S. Yan, and Y. Yang, Eur. Phys. J. C **66**, 187 (2010).
[40] S. Ryu and T. Takayanagi, Phys. Rev. Lett. **96**, 181602 (2006).
[41] S. Ryu and T. Takayanagi, J. High Energy Phys. 08 (2006) 045.
[42] J. M. Maldacena and G. L. Pimentel, J. High Energy Phys. 02 (2013) 038.
[43] B. Swingle and T. Senthil, Phys. Rev. B **87**, 045123 (2013).
[44] G. W. Gibbons, M. B. Green, and M. J. Perry, Phys. Lett. B **370**, 37 (1996).
[45] A. Kehagias and K. Sfetsos, Phys. Lett. B **456**, 22 (1999).
[46] H. Liu and A. A. Tseytlin, Nucl. Phys. **B553**, 231 (1999).
[47] A. Kehagias and K. Sfetsos, Phys. Lett. B **454**, 270 (1999); S. S. Gubser, arXiv:hep-th/9902155; S. Nojiri and S. D. Odintsov, Phys. Lett. B **449**, 39 (1999); K. Ghoroku, M. Tachibana, and N. Uekusa, Phys. Rev. D **68**, 125002 (2003).